Microturbulence at the front of supercritical quasiperpendicular shocks

L. Muschietti[1] **and B. Lembège**[2]

[1]SSL, University of California, Berkeley, CA-94720, USA, email:laurent@ssl.berkeley.edu

[2]LATMOS-UVSQ-IPSL-CNRS, Guyancourt, F-78280 France, email:lembege@latmos.ipsl.fr

Abstract

In supercritical shocks a fraction of the incoming ions is reflected at the steep front and stream across the magnetic field in the foot. The drift of the reflected ion beam versus the electrons can easily destabilize waves in the electron cyclotron frequency range. By means of linear analysis, we show that several Bernstein harmonics can be unstable, their number being proportional to the drift, yet limited by the ion beam's temperature. By means of electromagnetic PIC simulations restricted to the foot, we investigate the nonlinear characteristics of these waves. First, high cyclotron harmonics develop in good agreement with linear dispersion properties. Second, as the high $k-$modes saturate by trapping ions of the reflected beam, an inverse cascade occurs whereby the spectral power shifts toward lower $k-$modes to eventually accumulate on the first harmonic. The late phase showcases the development of a magnetic component to the spectrum that had so far been mostly electrostatic. It also showcases a significant energy transfer from the ion beam to the electrons which experience a marked increase in temperature.

1. Introduction

Ion reflection is the first step in a chain of processes leading to dissipation at supercritical shocks. Reflected ions at the shock's front enable streaming instabilities that are excited by the relative drifts between populations of incoming ions, reflected ions, and electrons. The unstable waves grow sufficiently to alter the particle distributions while reducing the free energy, which results in irreversible dissipation.

For quasiperpendicular shocks, the reflected ions' velocity is in large part directed at 90^0 to the magnetic field $\mathbf{B_0}$. In this geometry the plasma microinstability that is the easiest to destabilize in the foot of the shock is a variety of electron cyclotron drift instability. It is excited by the relative drift between the reflected ion beam and the electrons, and has the unstable waves propagating upwards perpendicularly to $\mathbf{B_0}$. This has been shown in 1D PIC simulations of the full shock [1] as well as in 2D simulations that allowed for wave propagation obliquely to $\mathbf{B_0}$, yet were restricted to the foot [2]. In the present study too we restrict ourselves to simulations in the foot, but extend the work to a more realistic parameter regime (large plasma to cyclotron frequency ratio, $\omega_{\rm pe}/\Omega_{\rm e} = 10$, and large mass ratio, $M/m = 400$). The much higher spatial resolution afforded by the present 1D electromagnetic simulations enables us to study in exquisite details the development of the instability. The typical timespan of the simulations is on the order of $100\ \Omega_{\rm e}^{-1}$ and the wavelengths comprised between the electron gyroradius $\rho_{\rm e}$ and the Debye length $\lambda_{\rm d}$.

Another important microinstability that can also be driven in the foot by a drift between electrons and ions across $\mathbf{B_0}$ is the modified two-stream instability (MTSI) [3, 2]. It requires the propagation angle to be off perpendicular so that the electrons can freely zoom along the magnetic field lines. Typically, the maximum growth is on the order of a fraction of the lower-hybrid frequency $\omega_{LH} = (m/M)^{1/2}\Omega_{\rm e}$ [3], which is quite slower than the growth of the electron cyclotron drift instability. We run our simulation for a total time comparable to the lower-hybrid period, so that effects of the MTSI are not adressed here.

2. Dispersion properties: linear approach

We suppose that the standard assumptions of an uniform plasma apply to the flat portion of the foot, and adopt a coordinate system in which the electrons are at rest while ion beam and ion core drift in opposite x-directions in a way such that the net current is zero. The electrons are taken as hot and magnetized with a thermal velocity $\rm v_{te} = (T_e/m)^{1/2}$ and a gyroradius $\rho_{\rm e} = \rm v_{te}/\Omega_e$. In their contribution to the susceptibility one can recognize the term

978-1-4244-6051-9/11/$26.00 ©2011 IEEE

for electron cyclotron Bernstein waves,

$$Q_{\mathrm{xx,e}} = -\frac{1}{k^2\lambda_{\mathrm{d}}^2}\left[-1+\Lambda_0(\eta)+2\sum_{\mathrm{n}=1}^{\infty}\Lambda_{\mathrm{n}}(\eta)\frac{\omega^2}{\omega^2-\mathrm{n}^2\Omega_{\mathrm{e}}^2}\right]. \tag{1}$$

Here Λ_{n} is the modified Bessel function, $\Lambda_{\mathrm{n}}(\eta) \equiv I_{\mathrm{n}}(\eta)\exp(-\eta)$, and its argument $\eta \equiv (k\rho_{\mathrm{e}})^2 = (\omega_{\mathrm{pe}}/\Omega_{\mathrm{e}})^2(k\lambda_{\mathrm{d}})^2$. Ions are taken as unmagnetized on the timescale considered. The beam has density $\alpha < 0.5$, thermal spread $\mathrm{v_{tb}}$ and drift $\mathrm{V_b}$, while the core has, respectively, $1-\alpha$, $\mathrm{v_{tc}}$, and $-\mathrm{V_c}$, where $\mathrm{V_c} = \mathrm{V_b}\,\alpha/(1-\alpha)$. Their contribution to the susceptibility reads

$$Q_{\mathrm{xx,i}} = -\frac{\alpha}{k^2\lambda_{\mathrm{d}}^2}\frac{\mathrm{T_e}}{2\mathrm{T_b}}Z'\left(\frac{\omega-k\mathrm{V_b}}{\sqrt{2}k\mathrm{v_{tb}}}\right)-\frac{1-\alpha}{k^2\lambda_{\mathrm{d}}^2}\frac{\mathrm{T_e}}{2\mathrm{T_c}}Z'\left(\frac{\omega+k\mathrm{V_c}}{\sqrt{2}k\mathrm{v_{tc}}}\right). \tag{2}$$

with Z the usual plasma dispersion function. For the perpendicular geometry where $\mathbf{B_0}$ points in the $z-$direction and the wavector $\mathbf{k}$ in the $x-$direction, the electrostatic dispersion relation reads simply $1 + Q_{\mathrm{xx,e}} + Q_{\mathrm{xx,i}} = 0$.

The instability is due to a coupling between electron cyclotron Bernstein modes and an ion acoustic mode carried by the beam [4, 5]. In a ω vs. k plot each branch up to the upper-hybrid is basically horizontal with a weakly negative slope, whereby the frequency of the branch labeled n is comprised between $n\Omega_{\mathrm{e}}$ and $(n+1)\Omega_{\mathrm{e}}$ at low $k\rho_{\mathrm{e}}$ yet tends to $n\Omega_{\mathrm{e}}$ at high $k\rho_{\mathrm{e}}$. Therefore, a Doppler-shifted acoustic beam mode, $\omega = k\mathrm{V_b} - k\mathrm{c_s}\alpha^{1/2}$ cuts all the branches in succession. Close to each intersection an instability is possible for a small range of wavenumbers. Figure 1(a) shows the growth of the cyclotron harmonics as obtained from numerically solving the electrostatic dispersion relation. The emission is thus expected to occur in discrete bands of frequency. Here we have assumed the following parameter values: $\omega_{\mathrm{pe}}/\Omega_{\mathrm{e}} = 10$, $\mathrm{V_b/v_{te}} = 1.5$, $\mathrm{T_b/T_e} = 0.25$ and $\alpha = 0.25$. An important aspect of the instability is that its growth is superior to that of the corresponding ion acoustic instability [5]. Suppose the electrons are 'demagnetized' and their orbits do not feel $\mathbf{B_0}$. The potential instability would then be the usual ion acoustic (IA) excited by the drift of the ion beam vs the electrons. However, for a beam with temperature $\mathrm{T_b/T_e} = 0.25$ there is hardly an instability as demonstrated in Figure 1(b). In fact, the ion acoustic waves become heavily damped for $k\lambda_{\mathrm{d}} > 0.5$. One has to consider a very cold beam with $\mathrm{T_b/T_e} = 0.01$ in order to obtain growths comparable with those of the cyclotron drift instability. The asterisks in panel (b) indicate the maximum growth rate for each frequency band shown in panel (a) and are reported here for comparison's sake.

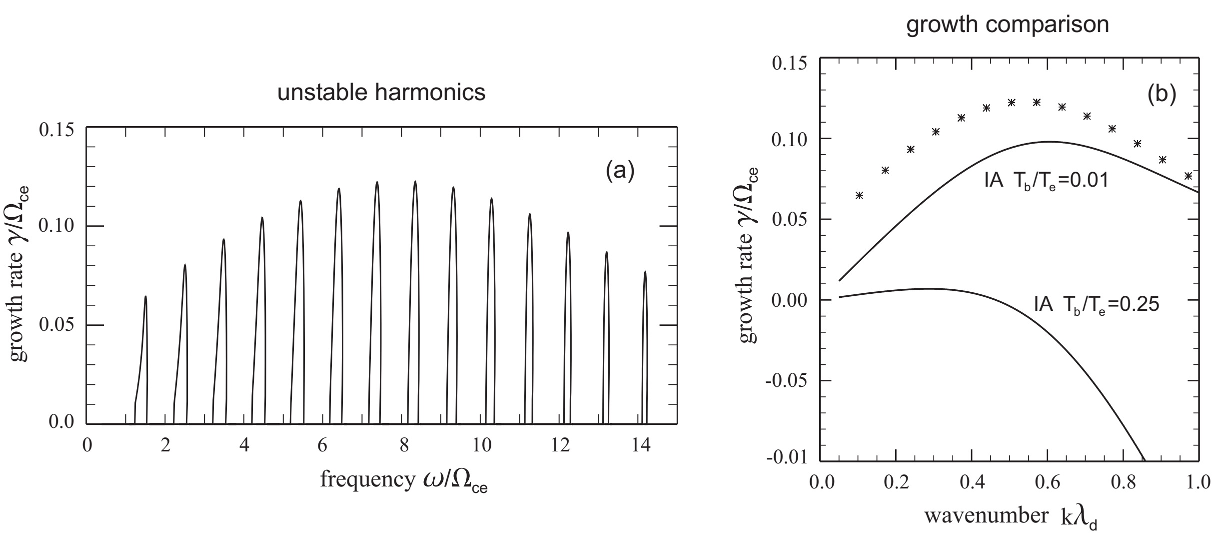

Figure 1: Growth rates for an ion beam drifting vs the electrons. (a) Narrow harmonic bands of frequency destabilized by the cyclotron drift instability with $\mathrm{T_b/T_e} = 0.25$. (b) Comparison with rates of the ion acoustic instability. Two temperatures are considered ($\mathrm{T_b/T_e} = 0.25$ and $\mathrm{T_b/T_e} = 0.01$). Asterisks indicate the maximum rate for each harmonic band displayed in (a).

3. Simulation results

The evolution of the instability has been investigated by means of 1D3V electromagnetic PIC simulations along the $x-$direction. In view of the spectral characteristics evidenced in the linear analysis the simulation box needs to have a length L sufficient to accomodate long wavelengths at the first harmonic and to yield $\Delta k = 2\pi/L$ small enough to resolve the narrow emission bands. Simultaneously, the cells themselves have to be sufficiently small to resolve features on the Debye scale.

Looking at the history of the electrostatic energy one can distinguish three successive phases. During the first phase, labeled "linear", the wave spectrum exhibits growth in bands of harmonics at high $k\rho_{\rm e}$ and high frequencies as expected from Figure 1(a). At very high wavenumbers, $k\lambda_{\rm d} > 0.5$ though, the growth is clearly inhibited by Landau damping on the ion beam. Figure 2(aa) shows a frequency spectrum typical of the first phase. The wave energy keeps on growing and saturate at the level $E^2/(4\pi n{\rm T_e}) \approx 10^{-3}$. During the second phase the wave spectrum becomes a mix of high and low $k\rho_{\rm e}$ modes. It is clearly a nonlinear regime marked with trapping of some beam ions by the high k modes whose growth is quenched. While the wave energy moderately decreases, one observes an inverse cascade that transfers the spectrum toward the low k modes. In the third phase, the spectral power accumulates on the first harmonic at $\omega \approx \Omega_{\rm e}$. The wave energy grows again to reach the level $E^2/(4\pi n{\rm T_e}) \approx 3 \times 10^{-3}$. We show a sequence of the electric signal in Figure 2(c) and a frequency spectrum typical of this late phase in Figure 2(cc).

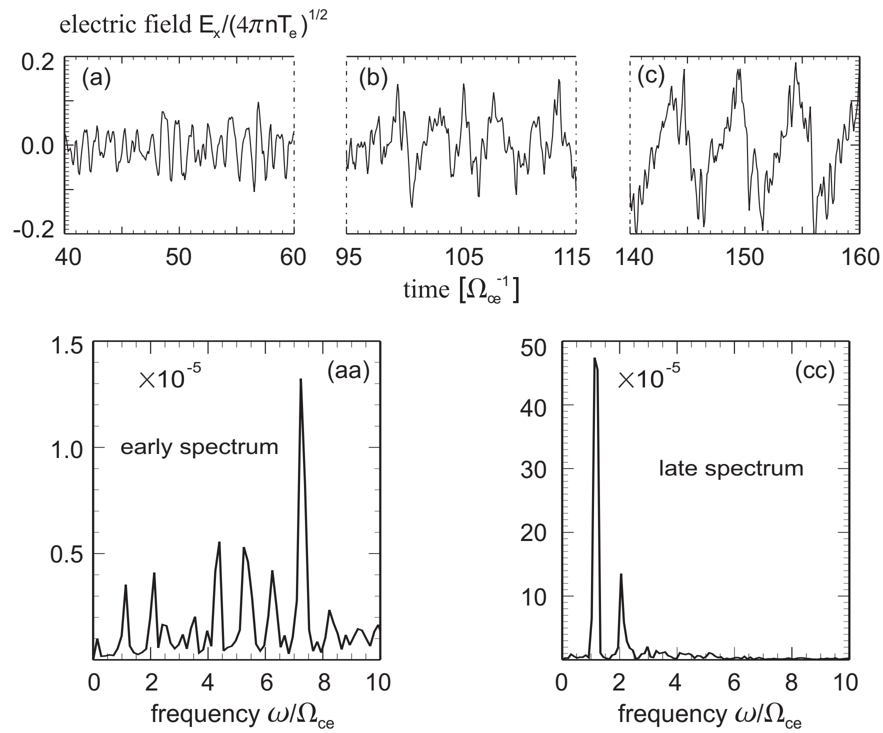

Figure 2: Electric signal recorded by a probe. (a)(b)(c) Successive time sequences recorded during the first, second, and third phases. (aa) Early spectrum with many excited harmonics. (cc) Late spectrum showing the accumulation of power on the first harmonic at the cyclotron frequency.

The third phase is characterized by the development of a magnetic component to the spectrum that had so far been mostly electrostatic. It also showcases a significant energy transfer from the ion beam to the electrons, which experience a marked increase in their temperature. Both features are related and may be understood by examining the motion of a cold electron in a wave with the extraordinary polarization. Recall that x is the direction of the wave electric field and z the one of the ambient magnetic field $\mathbf{B_0}$. While for $\omega >> \Omega_{\rm e}$ the orbit in $[x, y]$ space is mostly along x and for $\omega << \Omega_{\rm e}$ it is mostly along y, when the frequency is close to $\Omega_{\rm e}$, the orbit is elliptic with excursions in x and in y. This means that a current j_y is driven at the frequency of the wave, hence the observed magnetic signature δB_z. This also means that the distribution heats as electrons are extracted from the core and form a halo around it.

References

[1] L. Muschietti and B. Lembège, "Electron cyclotron microinstability in the foot of a perpendicular shock: A self-consistent PIC simulation", *Adv. Space Res.*, 37, 2006, pp. 483–493.

[2] S. Matsukiyo and M. Scholer, "On microinstabilities in the foot of high Mach number perpendicular shocks", *J. Geophys. Res.*, 111, 2006, pp. A06104–06114.

[3] C.S. Wu, Y.M. Zhou, S.T. Tsai, S.C. Guo, D. Winske, and K. Papadopoulos, "A kinetic cross-field streaming instability", *Phys. Fluids*, 26, 1983, pp. 1259–1267.

[4] H.V. Wong, "Electrostatic electron-ion streaming instability", *Phys. Fluids*, 13, 1970, pp. 757–760.

[5] M. Lampe, W.M. Mannheimer, J.B. McBride, J.H. Orens, K. Papadopoulos, R. Shanny, and R.N. Sudan, "Theory and Simulation of the Beam Cyclotron Instability", *Phys. Fluids*, 15, 1972, pp. 662–675.